Viability Study on Supervisory Control for a Solar Powered Train

Beatriz Féria and João Sequeira
Instituto Superior Técnico/Institute for Systems and Robotics, Lisbon, Portugal

Keywords: Solar Powered Train, Petri Nets, Supervisory Control, Energy Management System.

Abstract: This paper addresses the design and simulation of a control system for a solar powered train. An intelligent control approach using Petri nets is followed aiming at managing the energy consumption such that the train always reaches its destination. The system uses a priori information on the topology of the line, including length and slopes, locations of the intermediate stations, and also on the dynamics of the train, current solar irradiance and weather forecasting, and passenger weight, to determine bounds on the train velocity profile. The whole system was simulated integrating Petri nets in a Matlab/Simulink environment.

1 INTRODUCTION

This paper describes ongoing work under the framework of project Helianto (see (Helianto, 2013)) aiming at designing a multi-purpose solar powered light train. The paper describes a simulation environment built to assess the viability of the project.

The Helianto solar train is an autonomous vehicle, powered exclusively by solar energy and batteries. This makes it attractive for touristic purposes, connecting urban centers and environmentally sensitive areas. The train is equipped with an array of solar panels that can adjust their orientation in order to maximize the solar energy captured. The batteries onboard are recharged from the electric grid, whenever the train stops at a station, and using energy regenerated from braking.

Energy management systems have been extensively studied in a multitude of applications (Godoy Simaes et al., 1998; Jinrui et al., 2006). Route topology, predicted meteorological conditions and forces opposing the motion, gravity, rolling resistance and aerodynamic drag are examples on relevant conditions for project design, (Godoy Simaes et al., 1998) In order to develop the energy management system, all the components dealing with energy onboard the train and even those located on the outside, namely at the stations and along the railway line have to be modeled realistically. In the Helianto project, the overall system is modeled through discrete events systems (DES). DES have an elegant representation in the form of Petri nets, for which there are available powerful analysis tools (Moody et al., 1994; Davidrajuh, 2008; G. Cassandras and Lafortune, 2008) and for which supervisory controller design techniques allow an easy inclusion of constraints found in this type of application. In a sense,this is also resource management problem and Petri nets are reference tools to this class of problems, (Bogdan et al., 2006).

This paper is organized as follows. Sections 2 and 3 discuss some of the modeling options and simulation tools. Section 4 presents a Petri net model of the overall system, with the corresponding supervisory controller being described in Section 5. Simulation results are discussed in Section 6 and the conclusions of the paper are presented in Section 7.

2 INFRASTRUCTURE

The topology of the line and the placement of the stations placed along the line are assumed a priori known. The train uses GPS and the information on the topology of the line, eventually with a selection of landmarks placed along the line. Standard robotic sensors, e.g., laser range finders, can be used to detect obstacles. Also, an internet connection can be used to access short-term weather forecast services for the region where the train is operating, if available.

Each station can be equipped with a gate through which the passengers must go through to access the train. The gate system keeps count on how many people are in the station ready to board the train. Moreover, weight sensors at the gate floor allow to estimate the total weight to board the train at each station.

Féria B. and Sequeira J..
Viability Study on Supervisory Control for a Solar Powered Train.
DOI: 10.5220/0004422404230430
In *Proceedings of the 3rd International Conference on Simulation and Modeling Methodologies, Technologies and Applications* (SIMULTECH-2013), pages 423-430
ISBN: 978-989-8565-69-3

Given a time schedule for the train, specifying the arrival and departure times at each station, the goal of the supervisory controller is to generate a velocity profile reference such that (i) the train complies with the schedule, even in presence of abnormal events, (ii) the use of energy from the battery set is minimized, and (iii) the velocity and acceleration are always within operational limits defined by passenger comfort requirements. In case is not possible to find a solution the train must not start moving.

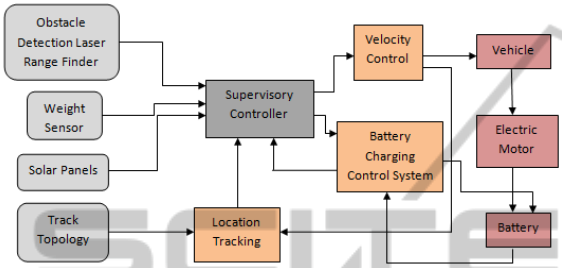

Figure 1: Block diagram of the overall system.

Figure 1 presents the block diagram for the global system.

Since it is a low-speed train, skidding is neglected and thus the dead-reckoning estimate can be fused, in the "Location Tracking" block, with GPS and landmark information using standard Kalman filtering techniques.

Once a reference velocity is generated by the corresponding block, the "Vehicle" block communicates to the "Motor" block the necessary torque which in turn generates the mechanical power required to move the train.

The batteries are kept at all times within an admissible range by the "Battery charging control" block . In case a minimum charge value is reached the block prevents further discharging and signals the system that the battery needs to be charged at the next station.

3 SIMULATION ENVIRONMENT

The simulation tool was developed under the Simulink environment with the toolboxes QSS, (QSS, 2008), to model the dynamics of the train, and Netlab, (Netlab, 2008), to construct a Petri net model of the system.

Netlab allows the design and graphical simulation of Petri Nets and can also interface Matlab/Simulink. Simulink imports a Netlab net as a single block. The exchange of data between the Petri net and the rest of the environment is reduced to the marking in input and output places.

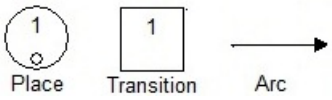

Figure 2: Netlab symbols for Petri nets.

Figure 2 illustrates the Netlab symbols used in the Petri nets. Supervisory control is then applied to the overall system through the Petri net block, establishing a direct, real-time, communication with Simulink.

The QSS toolbox simulates the behavior of a vehicle, motor and energy source, for given velocity and acceleration profiles, accounting, among others, for weight, wheel diameter, frontal area, friction and drag coefficients, and motor inertia. The velocity and acceleration profile is calculated based on information from the location tracking block, panels, and sensors. The track gradient profile is defined based on track topology and location tracking block. These inputs are assumed to be constant during each time interval, which for the purpose of this work was set to 1 second. At each step the torque required for the vehicle to follow the specified velocity profile is calculated, together with the necessary energy.

4 PETRI NET MODEL

4.1 Train

Figure 3a shows the Petri net modeling this subsystem. The main states are represented by places. A single token is passed on from place to place representing the current situation of the train. Once the train is ready, it starts moving when transition 1 is triggered, representing a start command. While moving two events can occur, the train enters a station (transition 5), or the laser detects an obstacle (transition 3). The first leads the train to stop and remain on a terminal state waiting to proceed to the next trunk. The second also leads the train to stop and wait for permission to finish the current trunk. These transitions can be assumed non-conflicting without loosing generality. In fact it is enough that obstacle detection range is longer than the length of the station approaching zone.

4.2 Motor

Figure 3b represents the Petri net that models the electric motor. There are four main operation modes for the motor and each one is represented by a place. The presence of a token in one of these places indicates the current mode of the motor. Once the motor is started

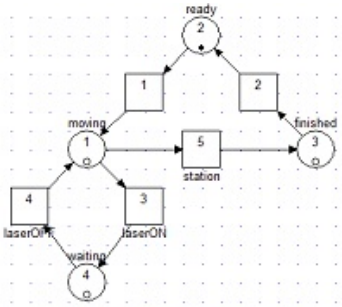

$$M_0=\begin{bmatrix} 1 & 0 & -1 & 1 & -1 \\ -1 & 1 & 0 & 0 & 0 \\ 0 & -1 & 0 & 0 & 1 \\ 0 & 0 & 1 & -1 & 0 \end{bmatrix} u_0=\begin{bmatrix} 0 \\ 1 \\ 0 \\ 0 \end{bmatrix}$$

(a) Petri net train behavior model.

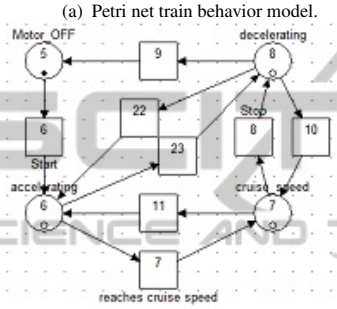

$$M_1=\begin{bmatrix} -1 & 0 & 0 & 1 & 0 & 0 & 0 & 0 \\ 1 & -1 & 0 & 0 & 0 & 1 & 1 & -1 \\ 0 & 1 & -1 & 0 & 1 & -1 & 0 & 0 \\ 0 & 0 & 1 & -1 & -1 & 0 & -1 & 1 \end{bmatrix} u_1=\begin{bmatrix} 1 \\ 0 \\ 0 \\ 0 \end{bmatrix}$$

(b) Petri net motor behavior model.

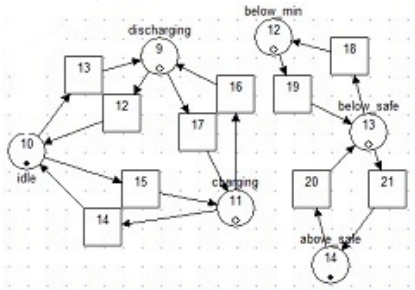

$$M_2=\begin{bmatrix} -1 & 1 & 0 & 0 & 1 & -1 & 0 & 0 & 0 & 0 \\ 1 & -1 & 1 & -1 & 0 & 0 & 0 & 0 & 0 & 0 \\ 0 & 0 & -1 & 1 & -1 & 1 & 0 & 0 & 0 & 0 \\ 0 & 0 & 0 & 0 & 0 & 0 & 1 & -1 & 0 & 0 \\ 0 & 0 & 0 & 0 & 0 & 0 & -1 & 1 & 1 & -1 \\ 0 & 0 & 0 & 0 & 0 & 0 & 0 & 0 & -1 & 1 \end{bmatrix} u_2=\begin{bmatrix} 0 \\ 1 \\ 0 \\ 0 \\ 0 \\ 1 \end{bmatrix}$$

(c) Petri net battery model.

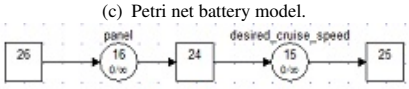

$$M_3=\begin{bmatrix} 1 & -1 & 0 \\ -1 & 0 & 1 \end{bmatrix} u_3=\begin{bmatrix} 0 \\ 0 \end{bmatrix}$$

(d) Petri net model for target velocity.

Figure 3: Petri net models for the main sub-systems and respective incidence matrices and initial conditions.

(transition 6) it accelerates until the vehicle reaches the referenced cruise velocity (transition 7). Once this happens the motor switches to cruise velocity mode. From this mode two possible events can occur: the vehicle stops (transition 8), and in that case the motor switches to decelerating mode or the vehicle is allowed to increase cruise velocity (transition 11) and in that case it switches to accelerating mode. Transition 8 can be set by three different types of events. The first occurs when the train approaches a station, then transition 8 fires leading the motor to decelerate until it stops. The second occurs when the laser range finder detects an object. If this happens the train is required to stop and transition 8 fires leading the vehicle to decelerate until it stops. In case the obstacle is no longer detected (transition 22) it is possible for the vehicle to switch from decelerating mode to accelerating mode in order to resume previous motion. Finally transition 8 can also be set by a power decrease event. If the output power of panels can no longer support current cruise velocity, transition 8 fires and the motor decelerates until a supported velocity is reached. It is also possible that this situation is reversed. This means that if the output power of panels increases, so does the supported cruise velocity and the motor switches to accelerating mode (transition 11) until it reaches the new cruise velocity.

4.3 Battery

The battery is modeled according to the stages of operation and the charge level condition (Figure 3c).

There are three possible stages of operation for the battery: idle, charging and discharging. If the power delivered by the panels is not enough to sustain minimum cruise velocity, the battery is allowed to discharge the necessary power so that the vehicle reaches that velocity. Also during accelerating mode, where a power peak demand occurs, the battery is allowed to discharge since the power requested during this mode is higher than the panels can deliver. If none of these situations occur, the battery remains in an idle stage waiting for a discharging or charging request.

The battery enters charging mode whenever the motor decelerates, through the regenerative braking system or at the stations, through the power grid, whenever the charge is below the safety value.

The battery condition is also modeled by three main states: above safety value, below safety value and below minimum value. The minimum value represents a characteristic property of each type of battery that states that the battery charge should never cross that threshold, at the risk of malfunction.

The safe value represents the necessary charge

that ensures the train reaches the next station considering situations such as low irradiance, obstacles on the track or even communication failure. At every station this minimum value must be met, charging the battery if necessary. If the battery charge remains between these two values, the token remains in the place representing below safe state.

4.4 Cruise Speed Reference

Figure 3d defines the desired cruise speed for the vehicle directly from the power delivered by the panels. Through transition 26, the marking of place 16 representing the panel is determined by Simulink. This means that the number of tokens in place 16 corresponds to the power delivered by the panels. The transfer of real measurements into the Petri net requires that those values are discretized and quantified into tokens. For instance, 1 token in place 16 means that the panels are delivering 1Kw power. The same reasoning is applied to velocity which means that 1 token in place 15 corresponds to a specific value cruise velocity for the vehicle. This calculation assumes that speed varies linearly with power. This linearity can actually be verified for low velocities such as the range considered for the solar train, (André, 2006).

5 SUPERVISORY CONTROLLER

The subsystems in Figure 3, that form the Helianto system are controlled by a supervisor, in charge of accounting for the constraints related to the resources and operation requirements. The approach followed in this work is that in (Moody et al., 1994). Roughly, it consists in describing the desired behavior for the supervisor through a set of linear constraints involving the marking and transition vectors.

A first version of the supervisor accounts for a basic set of constraints, listed below. This set does not yet account for temporal constraints such as the train timetable.

1. Once the battery crosses a minimum value threshold it stops discharging.
2. While the battery remains under minimum charge value, it cannot discharge.
3. The train is only allowed to begin traveling the next trunk in case the battery charge is above the safe value.
4. While the motor is at cruise speed mode it switches to decelerating mode when a station approaches or an obstacle is detected.

Table 1: Algebraic constraints and controller solution; v_i and u_j stand for the values of transitions and place markings, respectively.

Constraint	Description	Additional places	Additional arcs
1	$v_{14} \leq v_{20}$	place 19	–
2	$u_9 + u_{12} \leq 1$	place 18	–
3	$v_2 \leq u_{14}$	—	2
4	$v_8 \leq u_3; v_8 \leq u_4$	–	4
5	$v_6 \leq u_1$	–	2
6	$u_{15} \leq 4$	place 17	–

5. While the motor is off it only starts when the train is set to begin the next trunk or when an obstacle, causing the train to stop, is no longer detected.
6. Cruise speed cannot exceed a certain value.

The incidence matrix used corresponds to the global system matrix,

$$M = \begin{bmatrix} M_0 & 0 & 0 & 0 \\ 0 & M_1 & 0 & 0 \\ 0 & 0 & M_2 & 0 \\ 0 & 0 & 0 & M_3 \end{bmatrix}$$

where M_0, M_1, M_2 and M_3 are defined in Figure 3.

Table 1 summarizes the constraints as well as the controller places and arcs, on Figure 4, that result from each constraint.

The resulting supervised system is shown in Figure 4 where color (thick) arcs and places represent the controller elements added to the baseline model.

Accounting for a timetable can be done in multiple ways, e.g., (i) using a timed transition from place 7 to a new place so that the elapsed time can be counted through the marking of this new place, or (ii) simply add a new input place with the marking being defined after the events generated according to a real clock from Simulink. Each of these ways requires an active changing of the constraint that bounds the cruise velocity, in place 15, this meaning that a minimum cruise must be defined in order to the train meeting the schedule. The second of the aforementioned strategies was implemented and a new transition connected to a new place were added to the model. Since Netlab does not include timed transition elements, the transition is commanded by an external signal in Simulink that allows the firing whenever simulation time increases by one second. Once the transition fires a token is placed in the new place in order to account for the elapsed time. The same was applied to distance, and another transition and place were added to the model with the purpose of counting the covered distance. Both the covered distance and elapsed time signals are transferred to Simulink so that a minimum cruise velocity is defined for the train on a real-time basis.

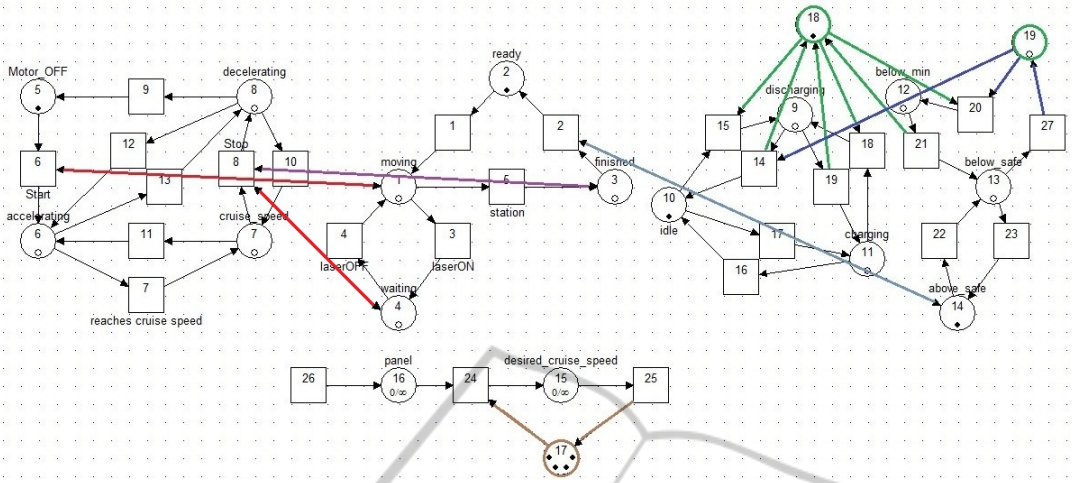

Figure 4: Petri net model of the supervised system.

6 SIMULATION RESULTS

This section presents simulation results obtained for the model designed in the previous sections. The performance of the train is analyzed for multiple scenarios and unpredictable events such as obstacle detection and unfavorable weather conditions. The performance of the train is evaluated based on energy consumption, time of travel and speed achieved. The power delivered by the panels varies along the day, depending directly on irradiance and on the suns' position. The irradiance of the sun along the day corresponds to the power delivered by the sun per square meter. The panels can only absorb part of this power, though is has to be taken into account that the efficiency depends on the technology and equipment. Currently the sunlight conversion rate (solar panel efficiency) in commercial products can go as low as 8.8% and as high as 43% for state of the art products, (SRoeCo Solar, 2013; State of California Energy Commission and California Public Utilities Commission , 2013). Throughout this section a value of 21% is assumed, corresponding to panels from a Japanese manufacturer sold in Europe.

The typical irradiance values can be obtained from a solar radiation data services website (SoDa, 2012). Since the main working season for the train is the Summer, the values used correspond to an average day in June as to consider the typical Summer irradiance conditions. Figure 5a shows the power delivered considering that the panels dimensions are 1.6x1m and that 12 panels are used. A maximum peak of around 4 kW can be obtained between noon and 2 pm. The relation between power and speed is considered linear (André, 2006), thus the corresponding equation is obtained by applying a linear interpolation between several velocities and corresponding power demand, given by QSS. The cruise velocity curve allowed for the train, given the time of the day and considering the power delivered at that time is also represented in Figure5a. A corresponding maximum velocity of 25 km/h can be reached during peak power. Considering the purpose of the Helianto project the minimum cruise velocity corresponds to 10 km/h. It is possible to observe that during summer months this velocity can be achieved from around 9 am to 5 pm. Until 9 am and after 5 pm the train requires the battery support in order to reach minimum cruise velocity. This requirement is assumed throughout the remaining simulations. Also, the average power delivered along the day is assumed to correspond to 3 kW.

An acceleration phase produces a power peak demand. The train is assumed to start with fixed acceleration and this value must be fixed to avoid unnecessary variations of energy demand and consequently unnecessary power peaks. A balanced acceleration value must be set so that the power peak can be sustained by the panels and battery. A range of acceleration values is tested as to define a suitable value at the start of the train. A typical urban train acceleration value corresponds to 1 m/s^2 which is considered comfortable from the point of view of the passenger (André, 2006). Since the solar train does not reach a typical range of speeds of an urban train, a possible range of acceleration values is considered from 0 to 1 m/s^2.

Figure 5b shows the energy consumption and power peak given a range of possible acceleration values. Cruise velocity was set at 20 km/h, the road gradient and weight carried are considered null and

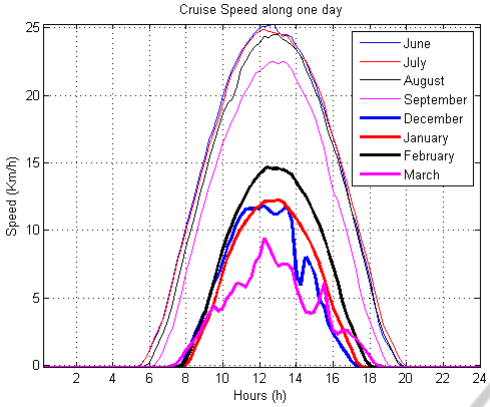

(a) Power delivered by panels and cruise velocity allowed along daytime.

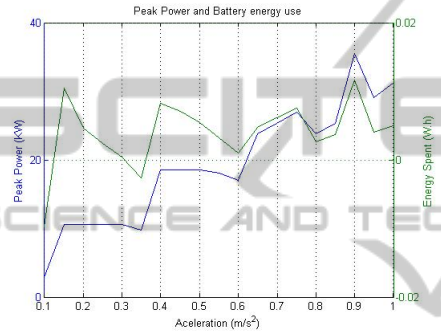

(b) Peak power and battery use vs. acceleration

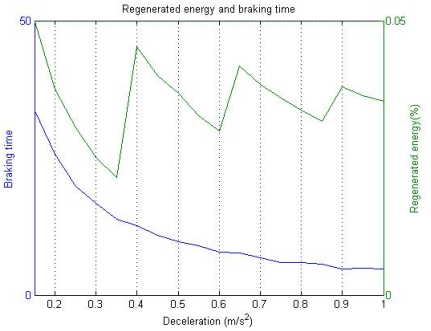

(c) Renegeration and braking time vs. deceleration

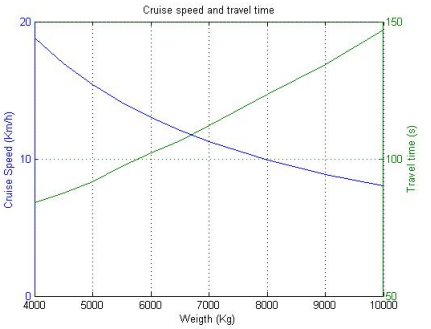

(d) Cruise speed allowed and travel time vs. weight carried by the train

Figure 5: Simulation results.

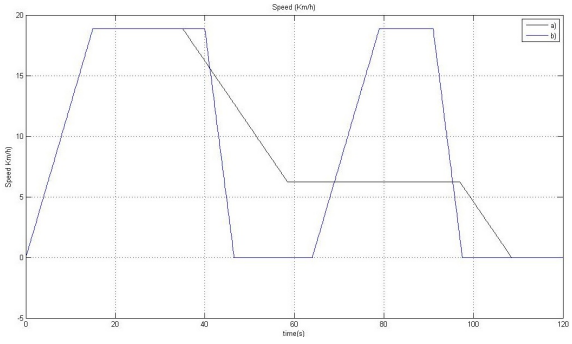

(a) Train speed vs. time.

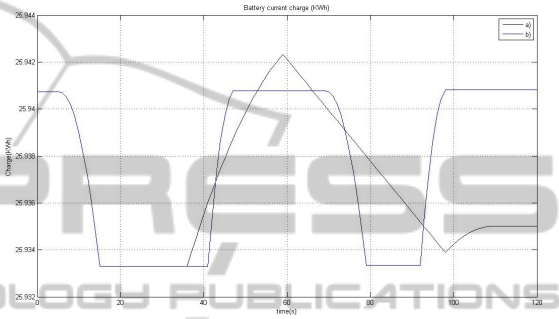

(b) Battery charge vs. time.

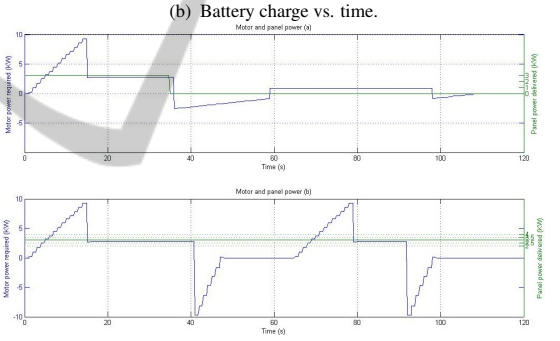

(c) Motor power required and panel delivered power for each scenario.

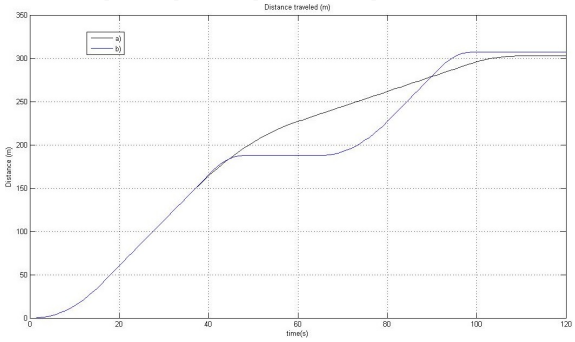

(d) Distance traveled by the train vs. time.

Figure 6: Simulation results for two scenarios: obstacle detection (b) and power cut (a).

the trunk length, braking deceleration, and panel delivered power are constant. As expected, the peak power increases with acceleration. Energy consumption is higher for the highest and lowest acceleration

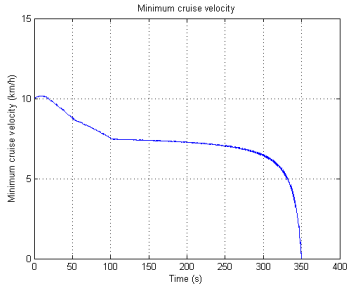

(a) Minimum velocity required to reach the target within schedule.

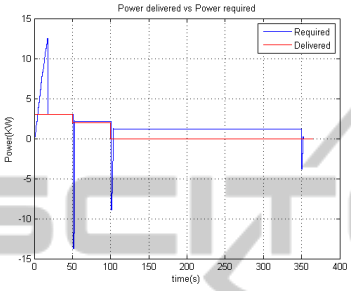

(b) Battery charge vs. time.

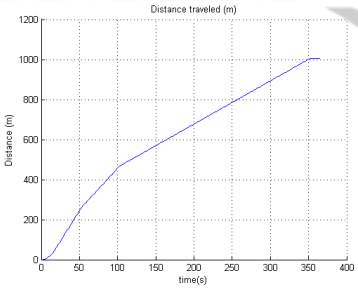

(c) Distance traveled by the train vs. time.

Figure 7: Simulation results for a timed mission.

values. This can be explained since for the highest values the peak power is higher and therefore more energy is spent during acceleration. On the other hand for the lowest values the peak power is lower but it takes more time for the train to reach cruise speed, so the acceleration period is longer. Acceleration values between 0.15 and 0.35 m/s^2 are often considered as the range representing a tradeoff between admissible power peaks, total energy consumption, and passengers comfort. Hereafter, an acceleration of 0.35 m/s^2 is assumed in all simulations.

Deceleration is also set to a constant value. Braking time and passengers comfort must also be considered so the deceleration value should not be too low nor too high respectively. The corresponding simulation results can be seen in Figure 5c for the energy regeneration and travel time given a range of possible deceleration values. Cruise velocity was set to 20 km/h and the track gradient and passenger weight are considered null. The absolute deceleration value was linearly increased in order to observe the regenerated energy and braking time evolution. As expected, braking phase duration decreases for higher deceleration values, this happens because the higher the deceleration value, the later the train brakes in order to stop at the station.

Regeneration increases with deceleration. Reasonable values for deceleration are often in the range -0.6 and -0.8 m/s^2. Hereafter, a deceleration of -0.8 m/s^2 is assumed.

Train weight influences the power demand and consequently the velocity of the train. Figure 5d shows travel time and cruise velocity given the weight carried by the train, considering the same amount of power available. It is possible to see that the higher the weight the lower the cruise velocity reached by the train. Consequently the travel time increases with weight. For a weight exceeding 8 tonnes it is possible to see that the cruise velocity is lower than the minimum value of 10 km/h and the train must use battery power in order to achieve minimum cruise velocity.

The results of two simulations on different scenarios are presented in Figure 6, namely a power loss that prevents the panels from delivering power (for instance, cloudy weather), and an obstacle is detected on the track. The train is intended to travel 1 km and the power delivered by the panels is 3 kW. The battery initial charge is set to 7 kWh.

Figure 6a shows the velocity plot for each simulation. For the obstacle scenario the train reaches cruise speed around time unit 15. At time 40, when the obstacle is detected, the train brakes to full stop. The obstacle detection is lost at time 65, when the train accelerates and reaches cruise speed again. Once it reaches final destination it decelerates again until it stops.

In this scenario it is also possible to see, Figure 6b, that the battery discharges only during acceleration and charges during deceleration, when regeneration occurs. During cruise speed the battery keeps its charge since the power delivered by the panels is able to support speed above minimum.

In the first scenario once the power loss is detected, the train decelerates until it reaches minimum speed. This speed guarantees the train reaches the destination within the time goal. This speed is supported exclusively by the battery, since the panels are delivering no power. Figure 6b shows that during this time the battery is discharging as expected, until the train approaches the station.

Figure 6c represents the power required by the motor and the power delivered by the panels. It is possible to see in Figure 6b that whenever the de-

mand is larger than the power delivered, the battery discharges. This is verified in the acceleration phase and also during the power cut, in order to support the minimum speed.

Figure 6d represents the distance traveled by the train during simulation. By comparing these graphics with the speed profile shown in 6a it is possible to see that the model is consistent.

Accounting for a time schedule was implemented by feeding the Petri net model with a timing signal from the external environment. A simulation was performed where the train is required to travel 1 km within a maximum time of 360 s. The results are shown in Figure 7.

Figure 7a shows the minimum velocity required in order to reach the target within the maximum time given. A higher velocity is allowed as long as the panels are able to sustain it. Through Figure 7b it is possible to see that until time 100 the panels are able to sustain a higher velocity, which causes the minimum velocity value to decrease as time passes. From that time instant forward the panels stop delivering power, which causes the train to assume the value of minimum velocity, in order to reach the target in time. The train travels at this velocity until it stops at the target within the defined schedule.

7 CONCLUSIONS

This paper describes a simulation tool to assess the viability of the Helianto solar train project.

The whole infrastructure was modeled as a discrete events system (DES), represented by Petri nets, and a supervisory controller was designed for the whole system. Two key toolboxes were used for these purposes, respectively, QSS and Netlab. The performance of the train is analyzed for multiple scenarios and evaluated based on energy consumption, travel time and speed achieved.

Simulations are performed on two different scenarios. The first scenario refers to a situation where an obstacle is detected on the track and the second refers to a power cut during travel. Temporal constraints such as the ones introduced by time schedules are also accounted for. The results were consistent, showing that the velocity achieved by the train allowed the motion to be maintained by the panels alone, resorting to battery only during acceleration phase, where a power peak demand occurs, or when a power failure occurs in order to sustain minimum velocity.

The results obtained show consistency in the sense that the train behaves as realistically expected and the energy consumption was effectively managed. Moreover, taking advantage of the flexibility of the Matlab/Simulink environment the overall tool is suitable for hardware-in-the-loop experiments.

ACKNOWLEDGEMENTS

This work was partially supported by FCT project PEst-OE/EEI/LA0009/2011.

REFERENCES

State of California Energy Commission and California Public Utilities Commission (2013). Go Solar California. http://www.gosolarcalifornia.ca.gov/equipment/pv_modules.php. Accessed January 2013.

André, J. (2006). *Transporte Interurbano em Portugal*, volume 2. IST Press. Lisbon (in Portuguese).

Bogdan, S., Lewis, F., Kovacic, Z., and Meireles Jr, J. (2006). *Manufacturing Systems Control Design: A Matrix Based Approach*. Springer.

Davidrajuh, R. (2008). Developing a New Petri Net Tool for Simulation of Discrete Event Systems. In *Procs. 2nd Asis Int. Conf. on Modeling and Simulation*.

G. Cassandras, C. and Lafortune, S. (2008). *Introduction to Discrete Event Systems*. Springer.

Godoy Simaes, M., Franceschetti, N., and Adamowski, J. (1998). Drive System Control and Energy Management of a Solar Powered Electric Vehicle. In *Procs. of the 13th Annual Applied Power Electronics Conf. and Exposition (APEC'98)*, volume 1.

Helianto (2013). The Helianto Project. Available at http://helianto.ist.utl.pt.

Jinrui, N., Fengchun, S., and Qinglian, R. (2006). A Study of Energy management System of Electric Vehicles. In *Procs. IEEE Vehicle Power and Propulsion Conf (VPPC'06)*.

Moody, J., Yamalidou, K., Antsaklis, P., and Lemmon, M. (1994). Feedback control of Petri nets based on place invariants. Lake Buena Vista.

Netlab (2008). Petri Net Toolbox: Netlab. Available at http://www.irt.rwth-aachen.de/en/fuer-studierende/downloads/petri-net-tool-netlab/.

QSS (2008). QSS-Toolbox. Available at http://www.idsc.ethz.ch/ Downloads/ qss.

SoDa (2012). SoDa, Solar Radiation Data. http://www.soda-is.com. Accessed January 2012.

SRoeCo Solar (2013). Most Efficient Solar Panels. http://sroeco.com/solar/most-efficient-solar-panels. Accessed January 2013.